FEBS Letters 519 (2002) 16–22 FEBS 26057

The determinants of the oligomeric structure in Hsp16.5 are encoded in the α-crystallin domain

Hanane A. Koteiche, Hassane S. Mchaourab*

Department of Molecular Physiology and Biophysics, Vanderbilt University, 1161 21st Ave. South, 741 Light Hall, Nashville, TN 37232, USA

Received 11 March 2002; revised 22 March 2002; accepted 27 March 2002

First published online 19 April 2002

Edited by Thomas L. James

Abstract The determinants of the oligomeric assembly of Hsp16.5, a small heat-shock protein (sHSP) from *Methanococcus jannaschii*, were explored via site-directed truncation and site-directed spin labeling. For this purpose, subunit contacts around the two-, three- and four-fold symmetry axes were fingerprinted using patterns of proximities between nitroxide spin labels introduced at selected sites. The lack of change in this fingerprint in an N-terminal truncation of the protein demonstrates that the interactions are encoded in the α-crystallin domain. In contrast, the truncation of the N-terminal domain of *Mycobacterium tuberculosis* Hsp16.3, a bacterial sHSP with an equally short N-terminal region, results in the dissociation of the oligomer to a trimer. These results, in conjunction with those from previous truncation studies in mammalian sHSP, suggest that as the α-crystallin domain evolved to encode a smaller basic unit than the overall oligomer, the control of the assembly and dynamics of the oligomeric structure became encoded in the N-terminal domain.

Key words: α-Crystallin domain; Hsp16.5; Hsp16.3; Small heat-shock protein; Electron paramagnetic resonance; Site-directed spin labeling

1. Introduction

Cells and organisms respond to heat shock and other forms of stress through the expression of multiple families of proteins referred to as heat-shock proteins (HSP) [1]. The small heat-shock protein (sHSP) superfamily consists of proteins with molecular weights less than 40 kDa per subunit that assemble into oligomeric structures of 4–40 subunits [2]. sHSP have emerged into the spotlight in recent years as a result of multiple genome sequencing projects that revealed their ubiquitous presence in all organisms and their constitutive expression in mammals, particularly in the lens, heart and the striated muscles [2–5]. While the reported spectrum of functions ranges from thermotolerance to regulation of apoptosis, in vitro sHSP recognize and bind unfolding proteins [6–10]. Given the species-specific pattern of abundance and expression, it is not unexpected that their cellular role has been optimized to the need of the organism.

From a structural perspective, recent studies suggest a considerable diversity at the oligomeric level, particularly between the evolutionarily distant members of the superfamily [11–15]. What is more striking is that the divergence in quaternary structure is accompanied by different degrees of order. Comparative cryogenic electron microscopy (cryo-EM) studies of Hsp16.5, α-crystallin and Hsp27 revealed a continuum from symmetric to variable assemblies [13]. Subunit exchange between oligomers in both αA-crystallin and Hsp27 was demonstrated by fluorescence resonance energy transfer [16,17]. Subunit exchange has been proposed to mediate the interaction with non-native states of proteins as well as membrane binding in lens α-crystallins [11,18].

The sequence and structural determinants of this polymorphism are less certain. Sequence similarity in sHSP is generally focused in a stretch of residues referred to as the α-crystallin domain, located in the C-terminal part of the sequence [2]. Thus, it was hypothesized that the highly variable N-terminal domain might be responsible for the divergence in the oligomeric structure [17,19]. However, recent studies on the tertiary structure of the α-crystallin domain in *Methanococcus jannaschii* (MJ) Hsp16.5 [14] and αA-crystallin [20] suggest a role for the α-crystallin domain in the diversity of the oligomeric structure. While confirming the presence of a core structure, the comparison also revealed the structural plasticity of this domain. This structural plasticity results in the formation of distinct dimers of the α-crystallin domain as building blocks of the oligomeric structure [20–22].

To better understand the evolution of structure and function of these proteins, our laboratory has studied representative sHSP from different species with the purpose of better defining structurally homologous regions and identifying the determinants of the diverse assemblies. Previous work employed a combination of truncation mutagenesis and site-directed spin labeling (SDSL) [23] to identify a conserved dimeric interface in Hsp27 and αA-crystallin [11]. The determination of the crystal structure of MJ Hsp16.5 [14] provides unique opportunities to extend these studies and better determine the role of the N-terminal domain in the assembly of the oligomer.

In this paper, using proximities in nitroxide pairs to fingerprint the quaternary structure of wild-type (WT) Hsp16.5, we demonstrate that the overall structure remains unchanged when the N-terminal sequence is removed suggesting that

*Corresponding author. Fax: (1)-615-322 7236.
E-mail address: hassane.mchaourab@mcmail.vanderbilt.edu (H.S. Mchaourab).

Abbreviations: sHSP, small heat-shock protein; MJ Hsp16.5, *Methanococcus jannaschii* heat-shock protein 16.5; WT, wild-type; MTSSL, methanethiosulfonate spin label; cryo-EM, cryogenic electron microscopy; SDSL, site-directed spin labeling; CD, circular dichroism

0014-5793/02/$22.00
PII: S0014-5793(02)02688-1

the determinants of oligomerization in this protein are entirely encoded in the α-crystallin domain. In contrast, truncation of the N-terminal domain of *Mycobacterium tuberculosis* Hsp16.3 [24] results in a species that migrates as a trimer on gel exclusion chromatography and in the loss of spin–spin interactions at site 103, shown previously to arise from the assembly of the trimer of trimers [11]. Taken together, these results in conjunction with previous studies [11,17] suggest a role for the N-terminal domain in defining the size, symmetry and perhaps the dynamic characteristics of the oligomer in mammalian sHSP.

2. Materials and methods

2.1. Materials

Methanethiosulfonate spin label (MTSSL) was obtained from Toronto Research Chemicals. Source Q media, Superose 6, Superdex 75, HiTrap Q and HiTrap desalting columns were obtained from Amersham Pharmacia Biotech. The POROS PEI column was obtained from Perkin Elmer. DNA oligonucleotides were purchased from Operon Technologies.

2.2. Site-directed mutagenesis

The two truncated α-crystallin domains of Hsp16.5 were constructed using the polymerase chain reaction (PCR). Two upstream primers were designed to include the *Nde*I restriction site flanking a 12-base sequence starting at codon 34 (TR1) and codon 42 (TR2), respectively. The 3′-primer was the T7 terminator primer. The PCR fragments generated were subcloned between the *Nde*I and *Xho*I sites of pET-20b(+) to yield the plasmids pET-t1HSP16.5 and pET-t2HSP16.5, respectively. The PCR fragments of single and double cysteine mutants were digested with the appropriate restriction enzymes and subcloned into both WT- and truncation 1-HSP16.5.

The two truncated α-crystallin domains of Hsp16.3 were constructed using PCR. The two upstream primers were designed to include the *Nde*I restriction site flanking a 12-base sequence starting at codon 31 (TR1) and codon 45 (TR2) respectively. The 3′-primer was the T7 terminator primer. The PCR fragments generated were subcloned between the *Nde*I and *Xho*I sites of pET-20b(+) to yield the plasmids pET-t1HSP16.3 and pET-t2HSP16.3, respectively. The single-cysteine mutant plasmids of native Hsp16.3, 91–95 and 101–104 [11], were digested with *Xma*I and *Xho*I and subcloned into the pET-t2HSP16.3 background.

2.3. Expression, purification and spin-labeling of the mutants

HSP16.5 truncations and mutant plasmids were used to transform competent *Escherichia coli* BL21 (DE3). Cultures inoculated from overnight seeds were grown at 37°C until $OD_{600} = 0.7–0.9$. The synthesis of Hsp16.5 variants was induced by the addition of 0.4 mM isopropyl β-D-thiogalactopyranoside. After 3 h induction at 37°C, the cells were harvested by centrifugation and resuspended into a lysis buffer containing 20 mM Tris, 1 mM EDTA, 100 mM NaCl and 10 mM dithiothreitol, pH 8. The resuspended cultures were then disrupted by sonication and the DNA precipitated by the addition of 0.06% polyethyleneimine. The lysates were then centrifuged at $15\,000 \times g$. Hsp16.5 variants were purified by anion exchange on a source Q column. Ammonium sulfate was added to the eluted anion exchange peak to a final concentration of 1 M, and the sample was then loaded on a phenyl Sepharose column. This step was followed by gel filtration chromatography on a Superose 6 column (buffer: 20 mM MOPS, 50 mM NaCl, 0.1 mM EDTA, pH 7.2). The sample was then reacted with a 10-fold excess of the MTSSL for 2 h at room temperature. The reaction was allowed to proceed to completion overnight at 4°C to yield the side chain R1 (Scheme 1).

Single-site mutants are named by specifying the original residue, the number of the residue followed by R1.

Hsp16.3 truncations and cysteine mutants were expressed and purified as described previously [11].

2.4. Reconstitution of mixed Hsp16.5 oligomers

Mutant proteins of MJ Hsp16.5 were mixed at a ratio of 1 to 3 with WT MJ Hsp16.5. Guanidine–HCl was added to a concentration > 5.5 M. The samples were incubated for 20 min at room temperature. They were then desalted into a buffer containing 20 mM MOPS, 50 mM NaCl, pH 7.2, and concentrated.

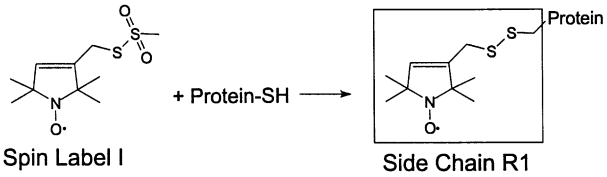

Scheme 1.

2.5. Electron paramagnetic resonance (EPR) measurements

The samples for EPR spectroscopy were prepared in 20 mM MOPS, 50 mM NaCl and 0.1 mM EDTA, pH 7.2. EPR spectra were collected on a Bruker E500 spectrometer equipped with a super High Q cavity. The microwave power was 2 mW, modulation amplitude was 1.6 G.

2.6. Circular dichroism (CD)

Far-UV CD measurements on Hsp16.5 and Hsp16.3, WT and truncations, were performed on a Jasco 720 spectropolarimeter at a concentration of 3 μM. Protein samples were prepared in 20 mM MOPS, 50 mM NaCl and 0.1 mM EDTA, pH 7.2. Measurements were taken in the range of 195–250 nm at room temperature.

2.7. Size-exclusion chromatography

The average molecular mass for all mutants was determined using size-exclusion spectroscopy. Hsp16.5 truncations and spin-labeled mutants were analyzed using a Superose 6 column and Hsp16.3 truncations were analyzed using a Superdex 75 column. All samples were injected from a 100 μl sample volume and a flow rate of 0.5 ml/min. The columns were calibrated before use with a set of known molecular weight proteins in the appropriate range.

3. Results and discussion

3.1. Truncation mutagenesis

Extensive sequence alignments [25] have defined a consensus sequence for the α-crystallin domain in sHSP. Residues preceding this domain are generally considered the N-terminal domain, although no conclusive evidence demonstrate that these sequences form independent folding units. In Fig. 1, the demarcations between the two domains in Hsp16.5 and Hsp16.3, suggested by de Jong et al. [25], are indicated by the arrows labeled 2. However, the crystal structure of Hsp16.5 [14] indicates that 10 residues flanking the sequence, forming a turn and a strand, are part of the α-crystallin domain in this protein (arrow 1 in Fig. 1). A secondary structure alignment of Hsp16.5 and αA-crystallin is also shown in Fig. 1. As pointed out previously, the α-crystallin domain in αA lacks the equivalent strands of β1 and β6 of Hsp16.5 [20].

Table 1
Molecular mass of R1-labeled mutants of Hsp16.5 WT and its N-terminal truncation 1

Residue	MW (MDa)	Residue	MW (MDa)
WT	0.42	TR1-WT	0.43
Q36R1	0.43	TR1-Q36R1	0.42
F42R1	0.44	TR1-F42R1	0.42
E101R1	0.42	TR1-E101R1	0.42
E102R1	0.42	TR1-E102R1	0.42
E103R1	0.42	TR1-E103R1	0.42
K110R1	0.41	TR1-E110R1	0.43
S46R1/S97R1	0.43	TR1-S46R1/S97R1	0.44
D51R1/R80R1	0.43	TR1-D51R1/R80R1	0.42

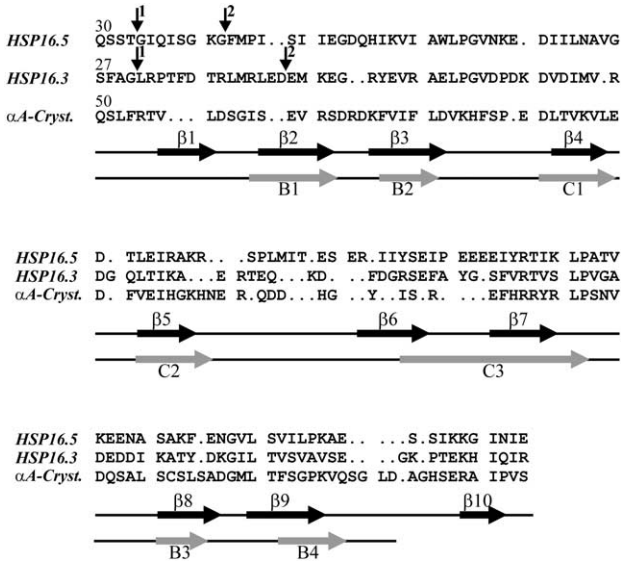

Fig. 1. Sequence and secondary structure alignment of the α-crystallin domain of HSP16.5, HSP16.3 and αA-crystallin according to de Jong and coworkers [21]. The black arrows, denoting β-strands (labeled β1–β10) refer to the secondary structure of HSP16.5. The gray arrows (labeled B1–B4, C1–C3) refer to αA-crystallin secondary structure. The arrows labeled 1 and 2 point to the residues at which the two truncations of Hsp16.5 and Hsp16.3 were constructed.

Accordingly, two sets of truncation mutants of Hsp16.5 and Hsp16.3 starting at the residues indicated by arrows 1 and 2 in Fig. 1, i.e. either with or without the β1 strand, were constructed. While both truncation mutants (1 and 2) of Hsp16.5 were expressed, consistently truncation 2 at residue 42 precipitated following anion exchange purification. The reverse behavior was observed for Hsp16.3. Truncation 1, starting at the beginning of the putative strand β1, was not detectably expressed while truncation 2 at residue 44 was overexpressed and easily purified, with no precipitation of the protein observed. Thus, in what follows, site-directed cysteine mutants of Hsp16.5 were introduced in the WT protein and in truncation 1 (residues 34–147), while those of Hsp16.3 were introduced in the WT protein and in truncation 2 (residues 45–144).

3.2. Oligomeric and secondary structure of truncated Hsp16.5

The effect of the removal of the N-terminal domain on the oligomeric structure was investigated using size-exclusion chromatography. Changes in apparent molecular masses, obtained against a set of proteins of known molecular masses, are an indicator of changes in the size and shape of the oligomeric assembly. Size-exclusion chromatography is particularly useful in cases where no changes are detected or dramatic reduction in the apparent masses are observed, both cases can be unequivocally interpreted. Table 1 reports the apparent molecular mass of the truncated Hsp16.5 and its spin-labeled mutants. The overall size of the oligomer is intact in truncated Hsp16.5, suggesting that no changes in the hydrodynamic radius result from the removal of the N-terminal domain.

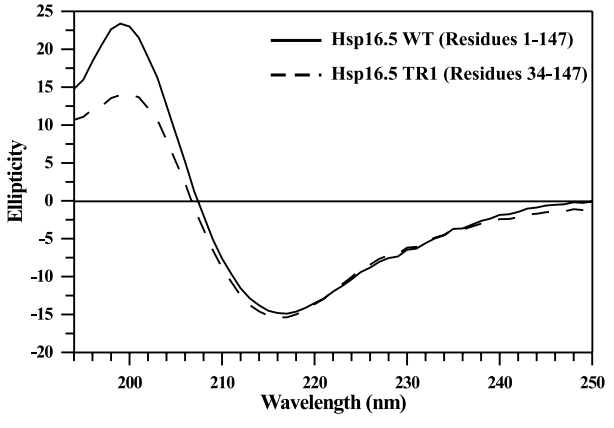

Fig. 2. Far-UV CD spectra of Hsp16.5 WT and truncation 1.

Far-UV CD reports on the overall content of secondary structure and was used to determine whether truncations of both proteins result in gross unfolding of the protein. In general, sHSP are characterized by a peak in ellipticity at or near 217 nm reflecting their β-sheet content as illustrated in Fig. 2 for WT Hsp16.5. More importantly, the removal of the N-terminal region did not affect the shape of the spectrum consistent with the α-crystallin domain being an independent folding unit and retaining its secondary structure.

3.3. The α-crystallin domain in Hsp16.5 encodes the determinants of the quaternary structure

3.3.1. Fingerprinting the quaternary structure of WT Hsp16.5 via internitroxide proximities. The crystal structure of Hsp16.5 has been reported by Kim et al. [14]. The oligomer consists of 24 subunits in contact around two-, three- and four-fold symmetry axes. From that perspective, the pattern of proximities between residues at the interfaces is a fingerprint of the quaternary structure. When introduced at subunit interfaces near the symmetry axis, nitroxides are brought into close proximity resulting in magnetic spin–spin interactions. The pattern of separation between the α-carbons results in a unique pattern of proximities between nitroxide spin labels introduced at these sites. The spin–spin interactions are reflected in the broadening and drop in the overall intensity of the continuous-wave EPR spectrum of the labeled oligomer relative to the corresponding spin-diluted oligomer. Spin dilution is achieved either by refolding the spin-labeled subunits in the presence of excess unlabeled WT or by labeling the subunits with sub-stoichiometric amount of spin label, both methods resulting in oligomers with predominantly a single spin-label at the interfaces. Fig. 3 is a slice through the structure of Hsp16.5 that shows all three axes of symmetry. For the purpose of illustration, an example of each class of sites selected for nitroxide labeling is highlighted.

Fig. 4 shows the EPR spectra of nitroxide pairs that fingerprint each of the subunit interfaces that define the oligomer. Qualitative analysis of the EPR spectra reveals that the internitroxide proximities are consistent with the crystal structure. For instance, the spectrum of F42R1, when compared to a spin-diluted oligomer, reveals strong spin–spin interaction consistent with a separation of less than 8 Å. The shape of the fully labeled oligomer continuous-wave EPR spectrum is characterized by spectral intensities separated by more than 120 G. It was not possible, for this mutant, to completely eliminate the interaction even by refolding in the presence of a four-fold excess unlabeled WT subunits. It appears that the destabilization of this mutant results in a less favorable interaction with WT subunits. Therefore, in the EPR spectrum of the spin-diluted oligomer, a minor second component with a

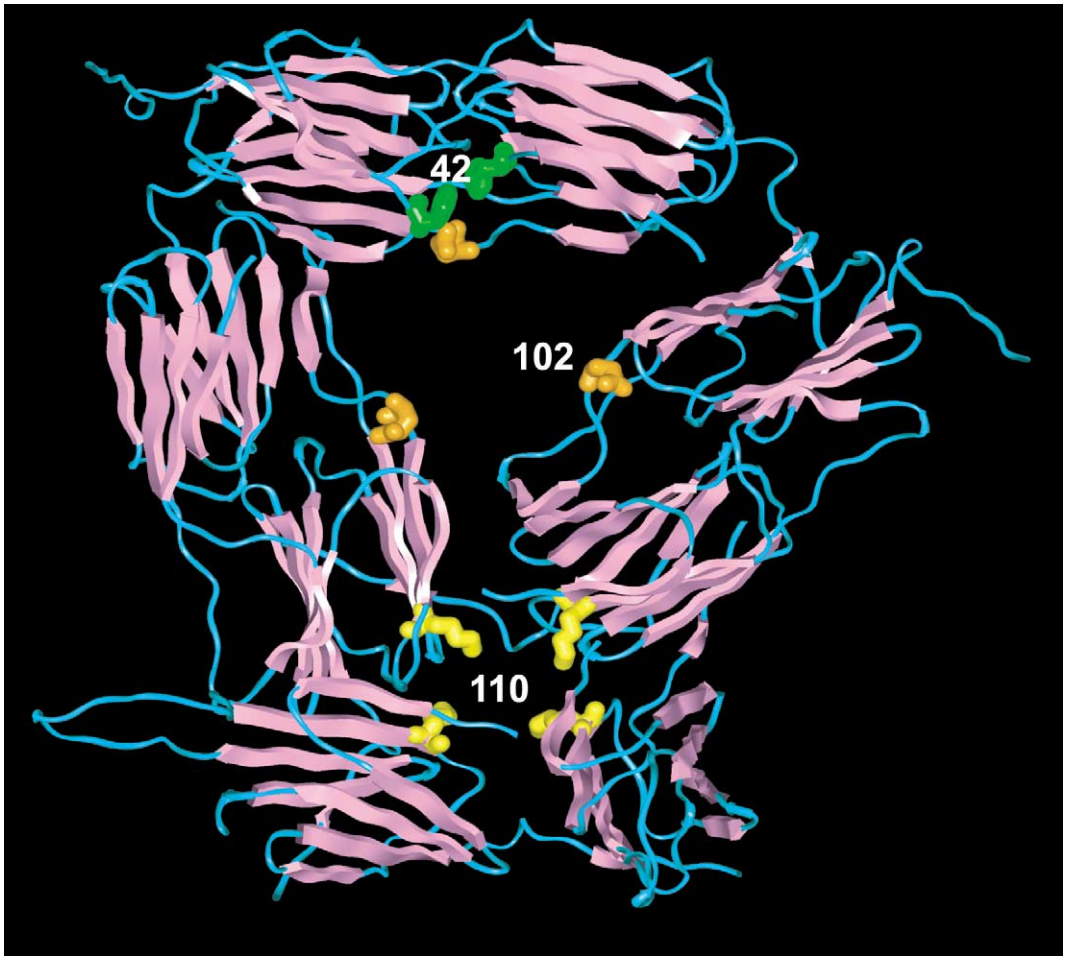

Fig. 3. Crystal structure of Hsp16.5 showing all three axes of symmetry. Representative residues are highlighted to illustrate the two-fold symmetry (residue 42), three-fold symmetry (residue 102) and four-fold symmetry (residue 110).

broad spectral width is observed. The broadening in the spectrum of the double mutant S46R1/S97R1 relative to the EPR spectrum obtained from the sum of the spectra of the single mutants reflects strong spin–spin interaction consistent with what is expected from the crystal structure. The sharp feature in this spectrum reflects a small (less than 10%) fraction of unreacted spin label. The two residues are brought into close proximity as a result of the swapping of strand β6 between monomers of Hsp16.5.

The spin–spin interaction observed at sites related by three-fold symmetry, i.e. residues 102 and 103, reflects the proximity between these residues in the oligomeric structure. The broadening in the fully labeled oligomer is in the intermediate range consistent with a 10–15 Å separation expected based on molecular modeling. Similarly, the three-fold symmetric interaction brings residues 51 and 80, each from a different monomer, into close proximity as revealed by the broadening in the EPR spectrum of the double mutant relative to that obtained from the sum of the spectra of the single mutants.

Finally, in the oligomeric structure of Hsp16.5, subunits make contacts around a four-fold symmetry axis. Consequently, residues such as K110 and Q36 from different subunits are in close proximity. As shown in Fig. 4c, the EPR spectra of R1 at these sites show considerable broadening relative to their spin-diluted oligomers consistent with the crystal structure.

3.3.2. Symmetry of the oligomeric α-crystallin domain.

Fig. 5 compares the EPR spectra obtained for the same spin-labeled mutants introduced in the truncated protein (TR1) (light trace) to those obtained in the WT protein (heavy trace). The EPR spectra of nitroxides introduced near the two-, three- and four-fold symmetry axes in both truncation and WT are almost superimposable demonstrating that the spectral features indicative of spin–spin interactions persist in the 34–147 residue truncation of Hsp16.5. This reflects a similar oligomer assembly both in the presence and absence of the N-terminal extension. Furthermore, aside from a small amount of unreacted label, the EPR spectra in the truncation are indicative of a rather homogeneous population. This is consistent with the lack of significant dissociation of the oligomer.

In conjunction with the size-exclusion data, these results demonstrate that in Hsp16.5, the α-crystallin domain assembles on its own into the native oligomer as defined by the crystal structure. Therefore, it encodes the determinants of the oligomeric structure.

3.4. N-terminal domain truncation of Hsp16.3 changes its oligomeric structure to a trimer

The absence of a high-resolution structure of Hsp16.3 precludes an extensive analysis similar to Hsp16.5. Yet several unique properties of this protein make it an interesting target

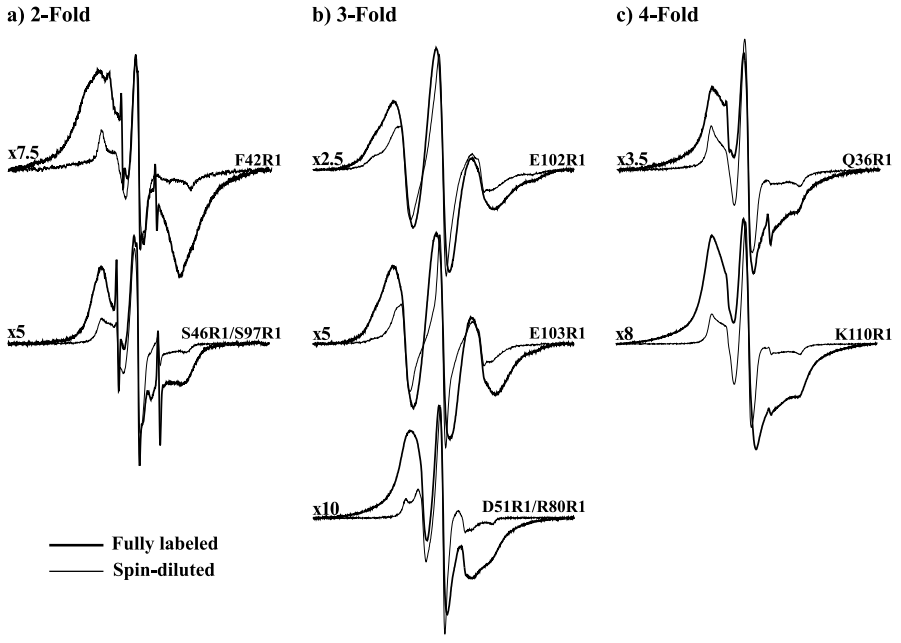

Fig. 4. EPR spectra of HSP16.5 mutants selected to fingerprint the two-, three-, and four-fold symmetry axis of the WT oligomer. The thick lines correspond to the fully labeled mutant and the thin lines correspond to the spin-diluted oligomer. All spectra are recorded with a 200 G scan width with the exception of the F42R1 spectrum which is recorded at 250 G and the E102R1 and E103R1 spectra recorded at 100 G. All are normalized to the same number of spins. The spectra of the fully labeled mutants are scaled to emphasize the drop in intensity. The scaling factor is shown to the left of the spectrum.

for mutational analysis. First, Hsp16.3 was the first sHSP reported to bind membranes [26], a property that is believed to be widespread in the superfamily [27]. Second, cryo-EM reveals two three-fold symmetry axes that suggest a nine-subunit oligomer [28]. A folding intermediate identified by size-exclusion chromatography and spin-labeling EPR is consistent with a trimeric building block for Hsp16.3. Berengian et al. [11] reported that residues 96–103 are located near a three-fold symmetry axis.

Removal of the N-terminal domain has quite different consequences in Hsp16.3 compared to Hsp16.5. A complete conversion to trimer is observed as revealed by size-exclusion chromatography suggesting that the interactions responsible for trimer formation are encoded in the N-terminal domain.

That the removal of the N-terminal region did not result in gross unfolding is demonstrated via comparison of the far-UV CD spectrum of the truncated protein with that of the WT. The spectra are superimposable reflecting a mainly β-sheet

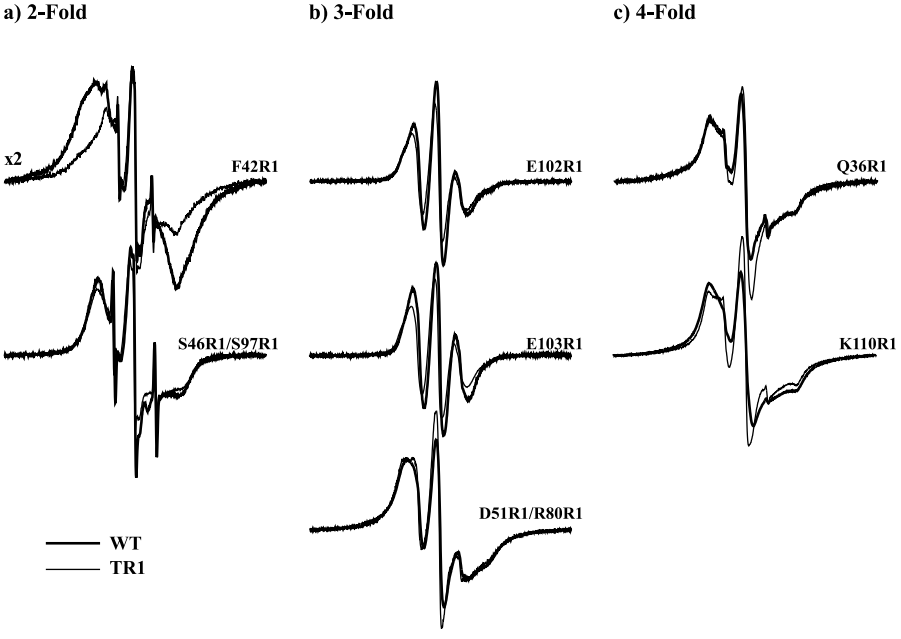

Fig. 5. EPR spectra of spin-labeled HSP16.5 mutants in WT (thick lines) and truncation 1 (thin lines). All spectra are recorded with a 200 G scan width and are normalized to the same number of spins with the exception of the F42R1 spectrum recorded at 250 G.

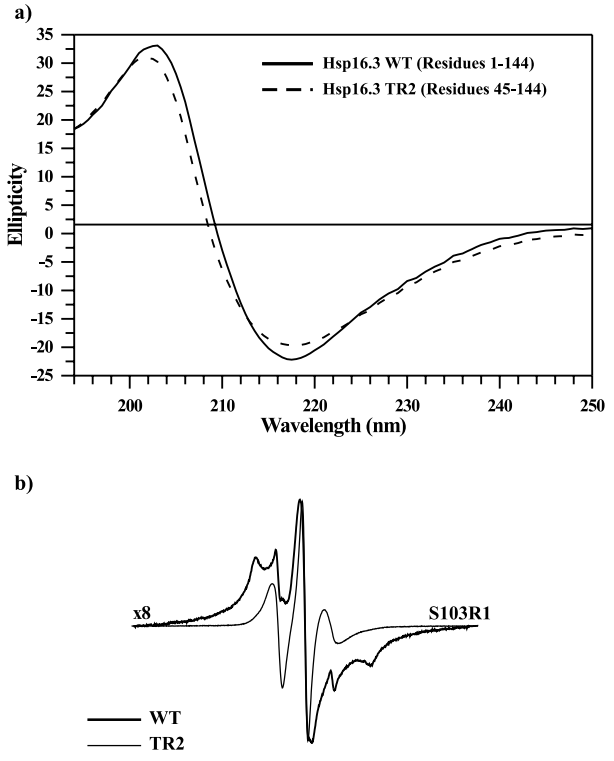

Fig. 6. (a) Far-UV CD spectra of HSP16.5 WT and truncation 2. (b) EPR spectra of the mutant S103R1. The thick line corresponds to the WT mutant while the thin lines correspond to the truncated mutant. The WT mutant spectrum is scaled to show the details of the lineshape.

structure (Fig. 6). The EPR spectra of the spin-labeled mutants 91–95 and 101–104 introduced in TR2, along the β-strand identified by Berengian et al. [11], reveal that the β-strand conformation of the backbone remains intact as expected (data not shown).

Previous EPR studies have revealed spin–spin interaction in the spectrum of R1 at site 103 of Hsp16.3 [11]. While this site is equivalent to site 110 in Hsp16.5, it was demonstrated that the origin of this interaction is the proximity of 103 to a three-fold rather than a four-fold symmetry axis. The EPR spectrum of R1, introduced into truncation 2 of Hsp16.3 at residue 103, shows no evidence of spin–spin interaction consistent with the conclusion of size-exclusion chromatography and in contrast to the results obtained at site 110 in Hsp16.5.

4. Conclusion

It is now well established that the α-crystallin domain forms a common structural core in sHSP [14,15,20]. What is less certain is the degree to which this domain defines the size, symmetry and degree of order for each oligomer. This communication demonstrates that in the predominantly ordered Hsp16.5 oligomer, this domain specifies all the interaction necessary for the assembly of the oligomeric structure. This is in contrast to αA-crystallin and Hsp16.3 and supports the contention that significant divergence has occurred in this domain to result in different subunit interactions.

The truncation of the N-terminal domain in αA-crystallin and Hsp27 also impairs subunit exchange in these proteins [17]. Thus, in light of the results of this paper a tantalizing hypothesis emerges with respect to the interplay between the roles of the N-terminal and C-terminal domains in mammalian sHSP. As the α-crystallin domain evolved to encode a smaller basic unit than the overall oligomer, the control of the assembly of the global structure became encoded in the N-terminal domain allowing a mechanism to modulate the oligomer dynamics. The interactions between subunits in the N-terminal domain are presumably weak enough for an association–dissociation equilibrium to be activated at physiological temperatures. The size of the N-terminal region, which tends to be larger in mammalian sHSP, is not significant since both Hsp16.5 and Hsp16.3 have about 30 amino acids in their N-terminal regions.

This hypothesis can also be used to answer a logical question that our results seem to raise concerning the need for an N-terminal extension in Hsp16.5. Cryo-EM studies have suggested that in solution even Hsp16.5 shows evidence of irregularly shaped particles [13]. Such polydispersity can be expected to be enhanced at the growth temperature of the organism, *M. jannaschii*. In this context, it is noted that our results do not rule out a role of the N-terminal region in modulating the stability of the oligomer. Studies under way to define the structure of this region which was not visible in the crystal structure suggest the presence of regular secondary structure and subunit contacts.

This paper further validates the use of SDSL to determine the oligomeric structure in sHSP. In every case, the spatial information deduced from the EPR spectrum was consistent with that expected based on the crystal structure, even at a buried site such as F42. In future studies, this approach can be used for a rapid screen for the presence of symmetries similar to Hsp16.5 in other members of the superfamily.

Acknowledgements: This work was supported by Grants EY12018 and EY12683 from the National Institute of Health.

References

[1] Parsell, D.A. and Lindquist, S. (1993) Annu. Rev. Genet. 27, 437–496.
[2] Caspers, G., Leunissen, J.A.M. and de Jong, W.W. (1995) J. Mol. Evol. 40, 238–248.
[3] Bhat, S.P. and Nagineni, C.N. (1989) Biochem. Biophys. Res. Commun. 158, 319–325.
[4] Klemenz, R., Fröhli, E., Steiger, R.H., Schäfer, R. and Aoyama, A. (1991) Proc. Natl. Acad. Sci. USA 88, 3652–3656.
[5] Vicart, P., Caron, A., Guicheney, P., Li, Z., Prevost, M.C., Faure, A., Chateau, D., Chapon, F., Tome, F., Dupret, J.M., Paulin, D. and Fardeau, M.A. (1998) Nature Genet. 20, 92–95.
[6] Horwitz, J. (1992) Proc. Natl. Acad. Sci. USA 89, 10449–10453.
[7] Lee, G.J., Roseman, A.M., Saibil, H.R. and Vierling, E. (1997) EMBO J. 16, 659–671.
[8] Jakob, U., Gaestel, M., Engel, K. and Buchner, J. (1993) J. Biol. Chem. 268, 1517–1520.
[9] Benndorf, R., Hayess, K., Ryazantsev, S., Wieske, M., Behlke, J. and Lutsch, G. (1994) J. Biol. Chem. 269, 20780–20784.
[10] Mehlen, P., Schulze-Osthoff, K. and Arrigo, A.P. (1996) J. Biol. Chem. 271, 16510–16514.
[11] Berengian, A.R., Parfenova, M. and Mchaourab, H.S. (1999) J. Biol. Chem. 274, 6305–6314.
[12] Haley, D.A., Horwitz, J. and Stewart, P.L. (1998) J. Mol. Biol. 277, 27–35.
[13] Haley, D.A., Bova, M.P., Huang, Q.L., Mchaourab, H.S. and Stewart, P.L. (2000) J. Mol. Biol. 298, 261–272.
[14] Kim, K.K., Kim, R. and Kim, S.-H. (1998) Nature 394, 595–599.
[15] van Montfort, R.L., Basha, E., Friedrich, K.L., Slingsby, C. and Vierling, E. (2001) Nature Struct. Biol. 8, 1025–1030.

[16] Bova, M.P., Ding, L., Horwitz, J. and Fung, B.K.-K. (1997) J. Biol. Chem. 272, 29511–29517.
[17] Bova, M.P., Mchaourab, H.S., Han, Y. and Fung, B.K. (2000) J. Biol. Chem. 275, 1035–1042.
[18] Cobb, B.A. and Petrash, J.M. (2002) Biochemistry 41, 483–490.
[19] de Jong, W.W., Leunissen, J.A.M. and Voorter, C.E.M. (1993) Mol. Biol. Evol. 10, 103–126.
[20] Koteiche, H.A. and Mchaourab, H.S. (1999) J. Mol. Biol. 294, 561–577.
[21] Mchaourab, H.S., Berengian, A.R. and Koteiche, H.A. (1997) Biochemistry 36, 14627–14634.
[22] Berengian, A.R., Bova, M.P. and Mchaourab, H.S. (1997) Biochemistry 36, 9951–9957.
[23] Hubbell, W.L., Gross, A., Langen, R. and Lietzow, M.A. (1998) Curr. Opin. Struct. Biol. 8, 649–656.
[24] Verbon, A., Hartskeerl, R.A., Schuitema, A., Kolk, A.H.J., Young, D.B. and Lathigra, R. (1992) J. Bacteriol. 174, 1352–1359.
[25] de Jong, W.W., Caspers, G.-J. and Leunissen, J.A.M. (1998) Int. J. Biol. Macromol. 22, 151–162.
[26] Lee, B.Y., Hefta, S.A. and Brennan, P.J. (1992) Infect. Immun. 60, 2066–2074.
[27] Cobb, B.A. and Petrash, J.M. (2000) J. Biol. Chem. 275, 6664–6672.
[28] Chang, Z., Primm, T.P., Jakana, J., Lee, I.H., Serysheva, I., Chiu, W., Gilbert, H.F. and Quiocho, F.A. (1996) J. Biol. Chem. 271, 7218–7223.